JOURNAL OF SOLID STATE CHEMISTRY **84**, 226–236 (1990)

Defect Ordering in $YBa_2Cu_3O_{6.5}$ and $YBa_2Cu_3O_{6.6}$: Synthesis and Characterization by Neutron and Electron Diffraction

Y. P. LIN, J. E. GREEDAN, A. H. O'REILLY, J. N. REIMERS,
AND C. V. STAGER

Institute for Materials Research, McMaster University,
Hamilton, Canada L8S 4M1

AND M. L. POST

Chemistry Division, N.R.C., Ottawa, Canada

Received June 28, 1989; in revised form October 9, 1989

Polycrystalline samples of $YBa_2Cu_3O_{6.5}$ and $YBa_2Cu_3O_{6.6}$ were prepared by oxygen titration of $YBa_2Cu_3O_{6.0}$ at 450°C followed by slow cooling to room temperature. Both samples showed evidence for the $a' = 2a$ supercell in individual grains by electron diffraction as reported previously. In addition the superlattice was observed in neutron powder diffraction indicating that the bulk material is also well ordered. In this study the $YBa_2Cu_3O_{6.6}$ phase showed longer correlation lengths for ordering along both a^* and b^* than $YBa_2Cu_3O_{6.5}$. For the former compound the powder-averaged, sample-averaged a^* correlation distance is 26 Å from neutron diffraction. Analysis of electron diffraction profiles on selected single crystals give correlation lengths along a^*, b^*, and c^* of 100, 200, and 50 Å, respectively. Dark field imaging discloses the presence of striped, ordered domains elongated along b^* with a distribution of sizes. Both neutron diffraction and dark field imaging indicate that the volume fraction of the ordered domains is about 50%. A correlation is noted between the Meissner Effect and the extent of defect ordering in the bulk samples of the two phases. © 1990 Academic Press, Inc.

Introduction

Much attention has been focused on the synthesis and characterization of oxygen-deficient $YBa_2Cu_3O_{6+x}$ since the earliest observations that about one oxygen per formula unit can be removed from the chain sites under relatively mild conditions (*1, 2*). Both experiment and theory indicate at least one phase intermediate between $x = 0.0$ and $x = 1.0$, namely, near $x = 0.5$, which is due to the ordering of oxygen vacancies. Experimentally, evidence for this intermediate ordered phase is manifest in the widely reported observation of a set of superlattice reflections of the type $(h/2\ 0\ l)$ in single crystals using electron diffraction and in one case X-ray diffraction (*3–6*). The currently accepted model for the ordered state involves alternating filled chains and vacant chains along the *b*-axis. This is consistent with the observed superlattice dimension $a' = 2a$ and minimizes the occurrence of three coordinate copper atoms.

Other evidence comes from the composition dependence of various physical properties such as the superconducting transition temperature, T_c, which shows a plateau at 60 K for the range $0.5 < x < 0.7$ which can be correlated with the existence

0022-4596/90 $3.00

of the $a' = 2a$ superlattice (*1*, *7*). Recent theoretical treatments also indicate a thermodynamically stable ordered phase near $x = 0.5$ (*8*).

Electron diffraction and related imaging techniques have been the primary experimental probes of defects in $YBa_2Cu_3O_{6+x}$ to date. This is due to the wide availability of electron microscopes and the high sensitivity of this method to the ordering of oxygen atoms. However, electron diffraction is restricted to observations on very small crystals which may or may not be representative of the bulk material on which analytical and physical data are measured and the diffracted intensities are difficult to interpret quantitatively. Neutron diffraction provides an excellent complement to electron scattering methods. While neutron sources are relatively weak and, thus, neutron scattering is somewhat less sensitive to defect ordering, the technique does probe the entire sample volume, so correlations with bulk analyses and properties are valid and the measured intensities are quantitatively useful.

We have thus undertaken neutron diffraction and electron diffraction/imaging studies on $YBa_2Cu_3O_{6+x}$ for well-characterized samples with nominal $x = 0.50$ and 0.60, i.e., the composition range where the superlattice is expected. To our knowledge there exist no published studies in which the oxygen ordering in these materials has been probed by both techniques in a complementary way.

Experimental

Sample Preparation and Characterization

Samples were prepared by a three-step process. First, $YBa_2Cu_3O_7$ was synthesized from stoichiometric quantities of Y_2O_3 (99.99%), $BaCO_3$ (99.999%), and CuO (99.999%) in alumina at 750–800°C. Following a 24-hr firing in air and subsequent regrinding and pressing into pellets (~2.5 g) the samples were annealed for an additional 48 hr in flowing oxygen followed by cooling to room temperature over 3 hr.

This material is then heated in vacuum to reach composition $YBa_2Cu_3O_{6.0}$ and then the oxygen content was adjusted to the desired composition by titration. These last two steps were carried out in a volume-calibrated stainless steel reactor (volume 7 cm^3) and vacuum manifold (29 cm^3) equipped with an oxygen and vacuum source and a high accuracy pressure transducer (Setra No. 204). The manifold was leak tested to better than 10^{-9} cm^3 atm (atm sec^{-1}). Effects of oxide formation or oxygen adsorption on the reactor walls were checked by introducing oxygen into the empty cell at operating temperatures.

Aliquots (~4 g) of sample were introduced into the reactor and the cell was evacuated ($p < 0.01$ Pa) while the temperature was raised to 1023 K, and held for 20 hr. After this treatment the sample was nominally $YBa_2Cu_3O_{6.0}$ as identified in preliminary experiments by chemical analysis and X-ray diffraction. Also, in preliminary experiments it was verified that no further oxygen could be removed by increasing the temperature to 1123 K and observing a negligible quantity of evolved gas.

The reactor temperature was then reduced to 723 K and aliquots of oxygen (typically 1.5 mmole) were added using the calibrated manifold as a gas titration apparatus. Two hours were allowed for equilibration following the addition of each aliquot. At the end of this interval the rate of O_2 transfer from gas to solid was less than 1 μmole hr^{-1}. Upon reaching the desired composition the reactor and sample were cooled to room temperature over a period of 2–3 hr. During cooling the quantity of O_2 absorbed was less than 0.5 mole O_2 corresponding to less than 0.03% of the total gas uptake.

Because of the need for large samples (~8 g) in the neutron diffraction experiments two samples of each composition were prepared. The actual compositions prepared here correspond to $x = 0.500(3)$ and $x = 0.600(4)$ in $YBa_2Cu_3O_{6.000+x}$ as determined by volumetric methods. Subsequently, the oxygenated samples were manipulated and transferred only under dry box conditions.

Trace elemental analysis by dc arc emission showed no evidence for contamination by the stainless steel vessel.

Lattice constants were determined from Guinier-Haag data and no impurity phases were observed in the product. The results are $x = 0.50$, $a = 3.836(5)$ Å, $b = 3.880(5)$ Å, $c = 11.75(2)$ Å; $x = 0.60$, $a = 3.832(2)$ Å, $b = 3.881(2)$ Å, and $c = 11.734(6)$ Å.

Analysis for oxygen content was performed by reducing the samples in a stream of dry hydrogen gas at 1000°C and observing the weight loss. Results for the nominal $x = 0.50$ and $x = 0.60$ samples were $x = 0.48(4)$ and $x = 0.65(4)$, respectively. Duplicate analyses were obtained which were reproducible to better than 0.15%.

Magnetic susceptibility data on both samples were obtained by use of a SQUID magnetometer from Quantum Design.

Neutron Diffraction

Neutron diffraction data were collected at the McMaster Nuclear Reactor using a powder diffractometer and a linear position-sensitive detector as described previously (*9*). Data were taken at 10 K using a closed cycle refrigerator with the sample contained in a thin-walled aluminum can filled with helium exchange gas and sealed with an indium wire gasket.

Electron Microscopy

Samples were prepared by grinding the powder material using a mortar and pestle. The crushed particles were loaded onto holey carbon films for examination in a Philips CM12 transmission electron microscope. Preliminary electron microscopy showed the presence of superlattice reflections due to cell-doubling in both $YBa_2Cu_3O_{6.5}$ and $YBa_2Cu_3O_{6.6}$ samples. The superlattice reflections were found to be streaked in the a^* direction and there was particle-to-particle variation in the intensity and degree of streaking. Part of this variation was thought to be caused by the use of a solvent during sample preparation for microscopy. Subsequently, samples were crushed and transferred in a dry nitrogen atmosphere without the use of any solvent.

Results and Discussion

Figure 1 shows the neutron diffraction powder pattern for the two compositions investigated here in the vicinity of the (0 0 2) reflection which itself is relatively weak, on the order of 1% of the strongest subcell reflections. Note that a reflection is observed at a lower Bragg angle than (0 0 2) for the sample $YBa_2Cu_3O_{6.60}$. This peak can be indexed as a ($\frac{1}{2}$ 0 0) reflection. A shoulder on the low angle side of (0 0 2) is also seen. In Fig. 2 the (0 0 2) subcell reflection has been subtracted to show the presence of this additional peak which can be indexed as ($\frac{1}{2}$ 0 1). Neither of these features appear in the powder data for a fully oxidized sample (not shown) but the weaker, sharper lines at higher angles are unchanged and these can be ascribed to $\lambda/2$ contamination of the beam. Attempts to fit these super cell reflections with a Gaussian line shape function showed that their FWHM was significantly greater than the (0 0 2) subcell reflection, by a factor of about 1.5, indicating a finite correlation length for ordering of the oxygen vacancies as had been reported in previous studies. Although there was some scatter in the data, an attempt was made to extract a correlation length by fitting a Lorentzian,

$$L(q) = \frac{1}{\xi^{-2} + q^2},$$

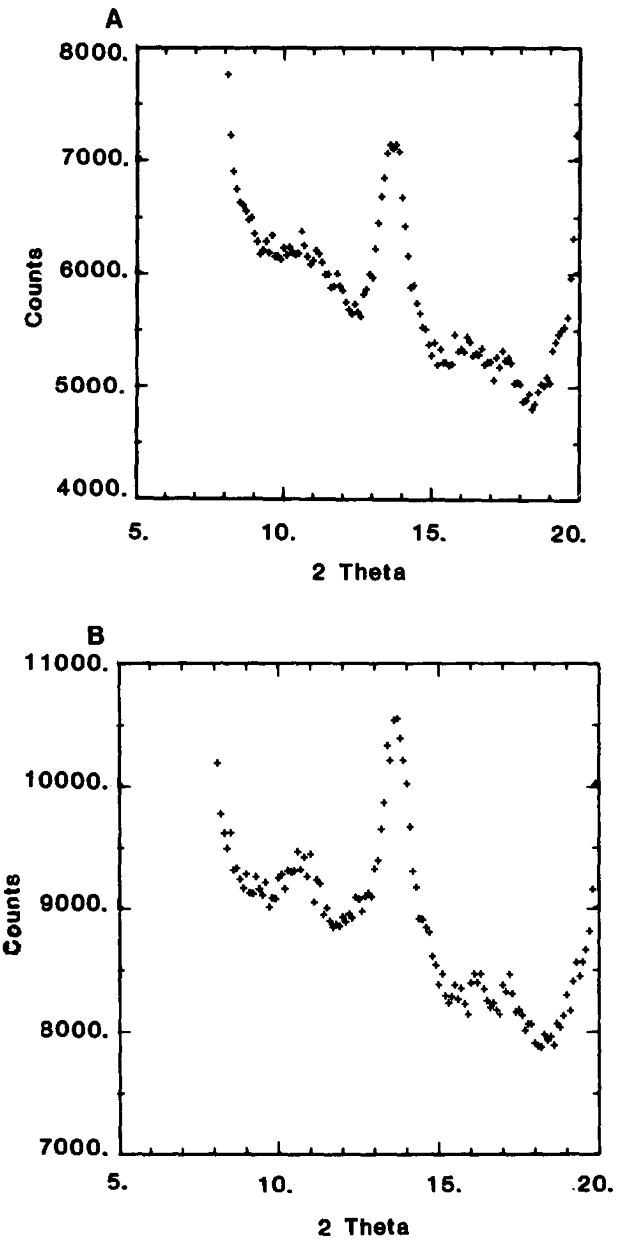

FIG. 1. Neutron diffraction powder pattern for $YBa_2Cu_3O_{6.5}$ (A) and $YBa_2Cu_3O_{6.6}$ (B) showing presence of weak ($\frac{1}{2}$ 0 0) peaks.

where ξ is the correlation length and q is the neutron scattering vector. This corresponds to assuming a 3-D Ornstein–Zernike correlation function in direct space of the form

$$C(R) = R^{-2} \exp(-R/\xi).$$

Since the half-width of the peak is on the order of the resolution half-width it is necessary to model the experimental peak

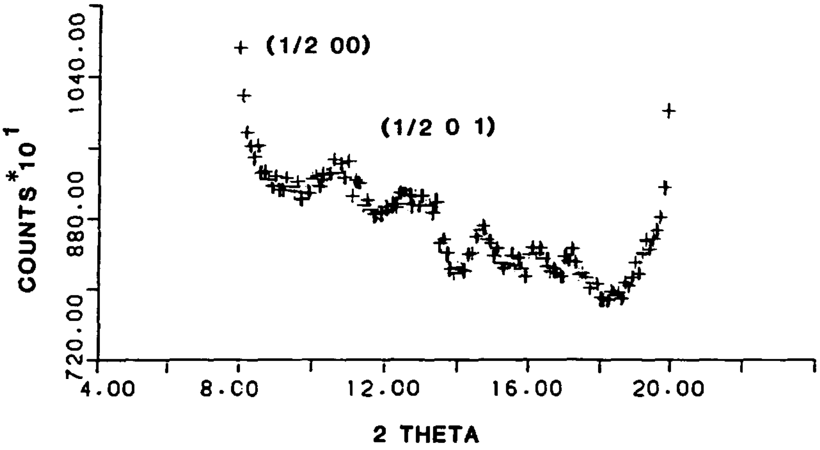

FIG. 2. Neutron diffraction pattern after subtraction of the (0 0 2) reflection showing presence of the ($\frac{1}{2}$ 0 1) reflection.

shape as a convolution of the Lorentzian $L(q)$ with the instrumental resolution function $R(q)$:

$$S(q) = \int_{-\infty}^{\infty} R(q')L(q - q')dq'.$$

In order to obtain an analytic expression for $S(q)$ the resolution function was approximated as a triangle with a half-width determined by fitting a Bragg peak.

Finally, the supercell peaks were fitted along with the neighboring Bragg peak assuming a linear background function. High correlations between background parameters, the intensity and ξ for the diffuse peaks resulted a relatively high degree of uncertainty in the final value of ξ, which was found to be 26(24) Å. Again, although the error is large the correlation length found here is of the same order as reported from earlier studies and it can be regarded as a sample-averaged value to compare with results from electron diffraction and dark-field imaging observations on individual grains of the same sample which will be described in another section.

The intensities of the supercell reflections can also provide an estimate of the volume fraction of the sample containing the ordered domains of the supercell. Table I shows the intensities of the observed supercell reflections relative to the (0 0 2) subcell reflection. The observed intensities are derived by fitting the profile to three Gaussians and a linear background function. These are compared with calculated values for ordered volume fractions of 1.0 and 0.50. The calculation for the 100% ordered structure is based on a doubled unit cell of composition $Y_2Ba_4Cu_6O_{13.2}$ with one set of fully occupied chain sites alternating with chain sites randomly occupied by 0.20 oxygen atoms. Atomic positions were derived from those found for the $YBa_2Cu_3O_{6.6}$ sub-

TABLE I

Relative Supercell/Subcell Intensities: Observed and Calculated Values

	Observed	Calculated (ordered vol. fraction)	
		1.00	0.50
$\frac{(\frac{1}{2}\ 0\ 0)}{(0\ 0\ 2)}$	0.20(4)	0.39	0.19
$\frac{(\frac{1}{2}\ 0\ 1)}{(0\ 0\ 2)}$	0.36(4)	0.55	0.28

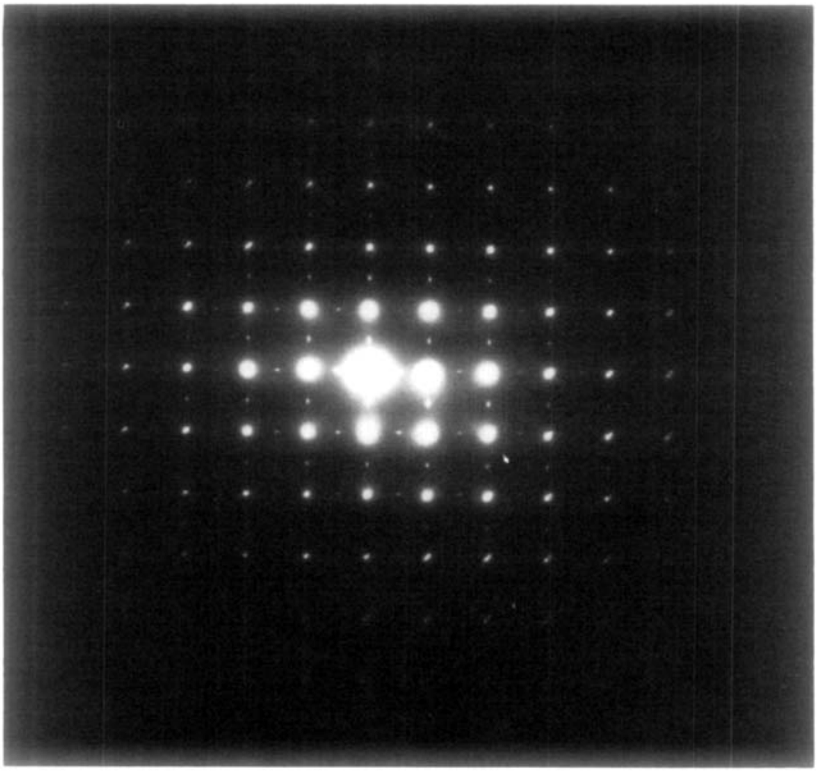

FIG. 3. [001] orientation electron diffraction pattern for $YBa_2Cu_3O_{6.6}$ showing streaking of superlattice reflections along *a*.

cell. The 0.50 vol fraction model is obtained by assuming fully ordered domains in a fully disordered matrix. This model is supported by the dark field imaging observations. The ordered volume fraction is seen to be about 0.50.

The supercell reflections from the $YBa_2Cu_3O_{6.50}$ sample are considerably weaker and broader than for our sample of $YBa_2Cu_3O_{6.60}$. This is somewhat surprising as the former composition is ideal for formation of the $a' = 2a$ superlattice. Although both samples were prepared under identical conditions it is possible that cooling rates or other sample history effects play a role in vacancy ordering and it is not obvious that this observed difference in the degree of defect ordering is intrinsic to the two compositions studied. Attempts to obtain intensities from these data were not successful.

In accord with the neutron diffraction results, the intensity of the superlattice reflections in electron diffraction patterns was found to be weaker and the streaking more pronounced in the $YBa_2Cu_3O_{6.5}$ sample than in $YBa_2Cu_3O_{6.6}$. Examples of typical [001] selected area diffraction patterns for the $YBa_2Cu_3O_{6.6}$ and $YBa_2Cu_3O_{6.5}$ samples are shown in Figs. 3 and 4, respectively. The streaked ($h/2$ k 0) reflections suggested that the ordered regions were quite small in the [100] direction. Both patterns show superlattice reflections from two sets of twins because the diameter of the area selection aperture was equivalent to about 200 nm of the specimen plane, so

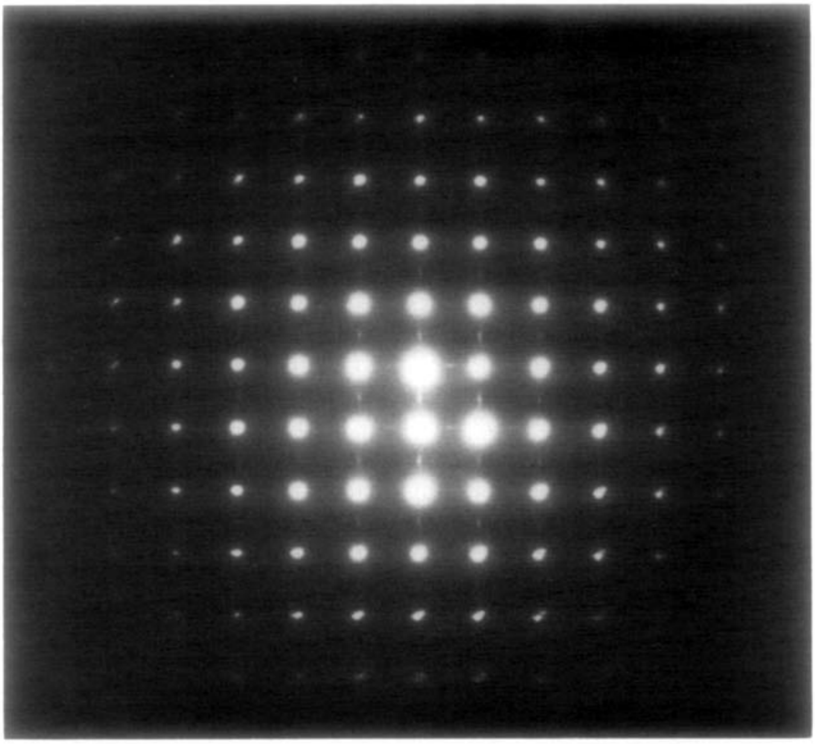

FIG. 4. [001] orientation electron diffraction pattern for $YBa_2Cu_3O_{6.5}$ showing pronounced streaking of superlattice reflections.

that more than one twin (typically 100 nm wide) was usually selected. Also, care was taken to ensure that an intense beam was not focused on the sample as beam heating generally resulted in the removal of the superlattice structure. In the present work, only the superlattice reflection due to cell doubling has been observed. Other intermediate phases produced by deliberate *in situ* heating experiments as reported by Reyes-Gasga *et al.* (*11*) have not been observed.

For the $x = 0.6$ sample, diffraction patterns from the [010] orientation have also been obtained (Fig. 5). In this section of the reciprocal lattice, the superlattice reflections (of the type $h/2\ 0\ l$) were found to be streaked in the c^* direction. Figures 3 and 5 thus indicate a ribbon-like shape for the superlattice reflections and a correspondingly ribbon-like shape (small in [100] and [001] but extended along [010]) for the ordered region in real space. The sizes of the ordered domains were estimated from the intensity profiles of superlattice reflections. Reflections from [010] and [001] patterns were digitized directly from the photographic negative using a microdensitometer and intensity profiles were obtained for each reflection along as well as perpendicular to the streaking direction (Fig. 6). The background was deduced from both profiles and the mean domain dimensions were taken to be that corresponding to the width at half-peak height (*10*). Without taking the effect of beam convergence and nonlinear effects in the photographic process into consideration, the domain sizes were found to be typically ~100, ~200, and ~50 Å in the a^*, b^*, and c^* directions, respectively.

Since the superlattice reflections in the

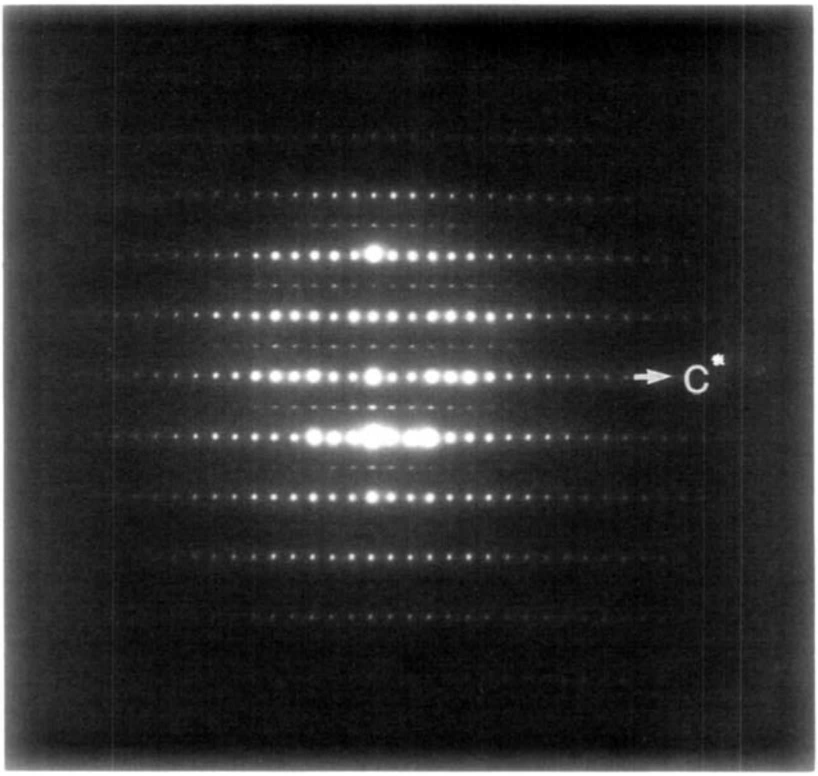

FIG. 5. [010] orientation electron diffraction pattern for $YBa_2Cu_3O_{6.6}$ showing streaking of superlattice reflections along *c*.

$YBa_2Cu_3O_{6.6}$ sample were reasonably strong, a crystal which showed somewhat sharper superlattice reflections than those shown in Fig. 3 was chosen and imaged in dark field using a ($h/2$ 0 0) reflection. The image (Fig. 7) showed domains of ordered regions (bright patches) present inside one set of twins. As expected from the intensity profiles, the domains appeared as narrow in the a^* direction and elongated in the b^* direction. The domain sizes showed considerable variation. For example, a domain size of up to 1000 Å along b^* can be observed in Fig. 7. Nevertheless, the size of the domains in the image seems to be in general agreement with the average sizes and aspect ratios estimated from intensity profiles. A visual inspection of Fig. 7 suggests that the area fraction of the ordered region is around 50%, indicating a corresponding volume fraction. This is consistent with the estimate from neutron diffraction data.

The pronounced streaking of the superlattice reflections in the $x = 0.5$ sample indicated that the domain sizes were smaller than in the $x = 0.6$ sample. Intensity profiles of reflections in the [001] pattern (Fig. 6) were rather irregular, particularly along the streaking direction (a^*) and may be indicative of a large variation in the domain size. From the intensity profiles, the average domain sizes were estimated to be ~40 and ~80 Å in the a^* and b^* directions, respectively. Since the superlattice reflections in this sample are weaker than in the $x = 0.6$ sample, dark field imaging was not attempted.

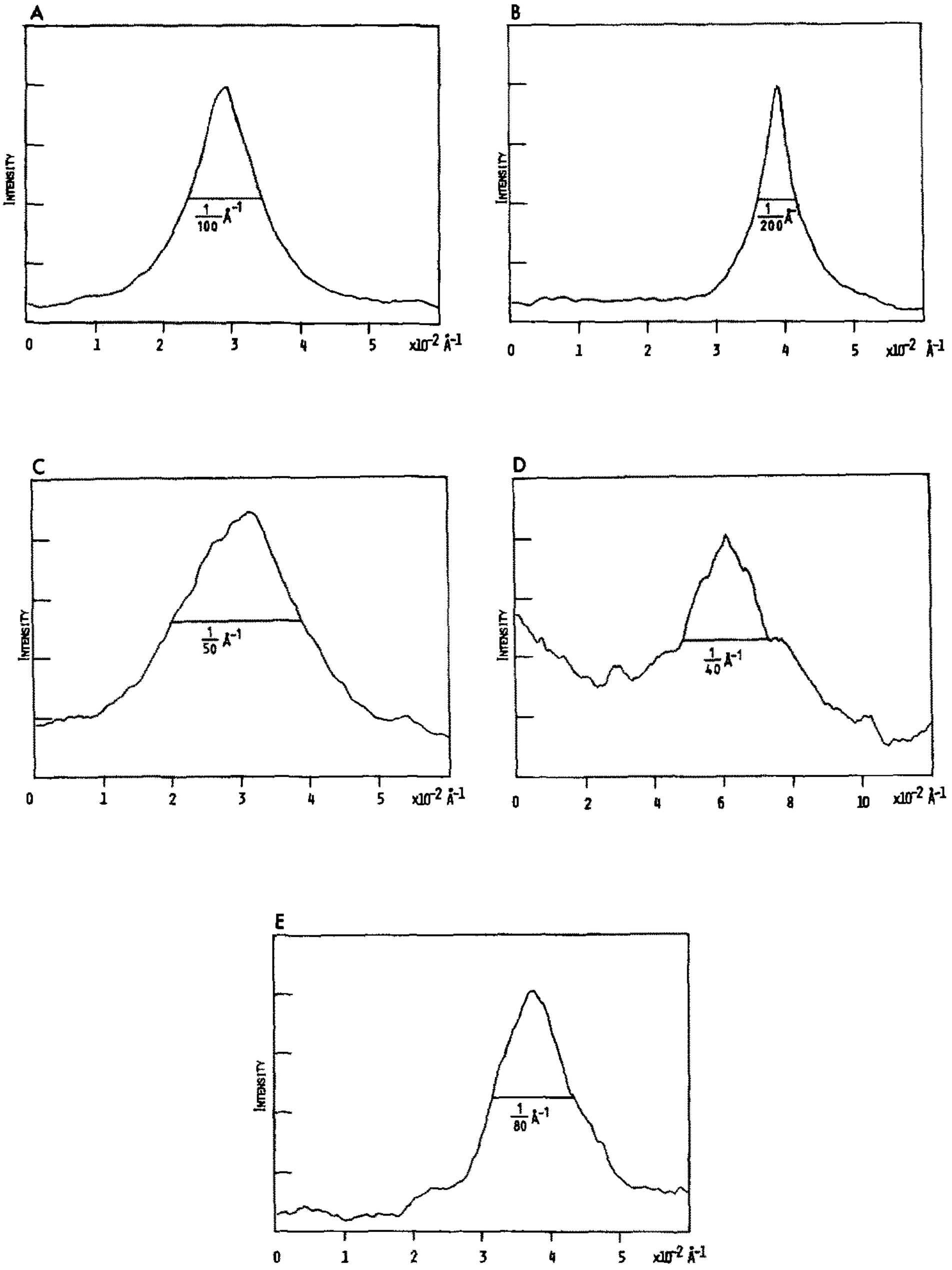

FIG. 6. Intensity profiles for superlattice reflections for (A) $YBa_2Cu_3O_{6.6}$ along a^*; (B) $YBa_2Cu_3O_{6.6}$ along b^*; (C) $YBa_2Cu_3O_{6.6}$ along c^*; (D) $YBa_2Cu_3O_{6.5}$ along a^*; and (E) $YBa_2Cu_3O_{6.5}$ along c^*. The intensity scale is arbitrary and the position scale is in units of 4.3×10^{-4} Å^{-1}.

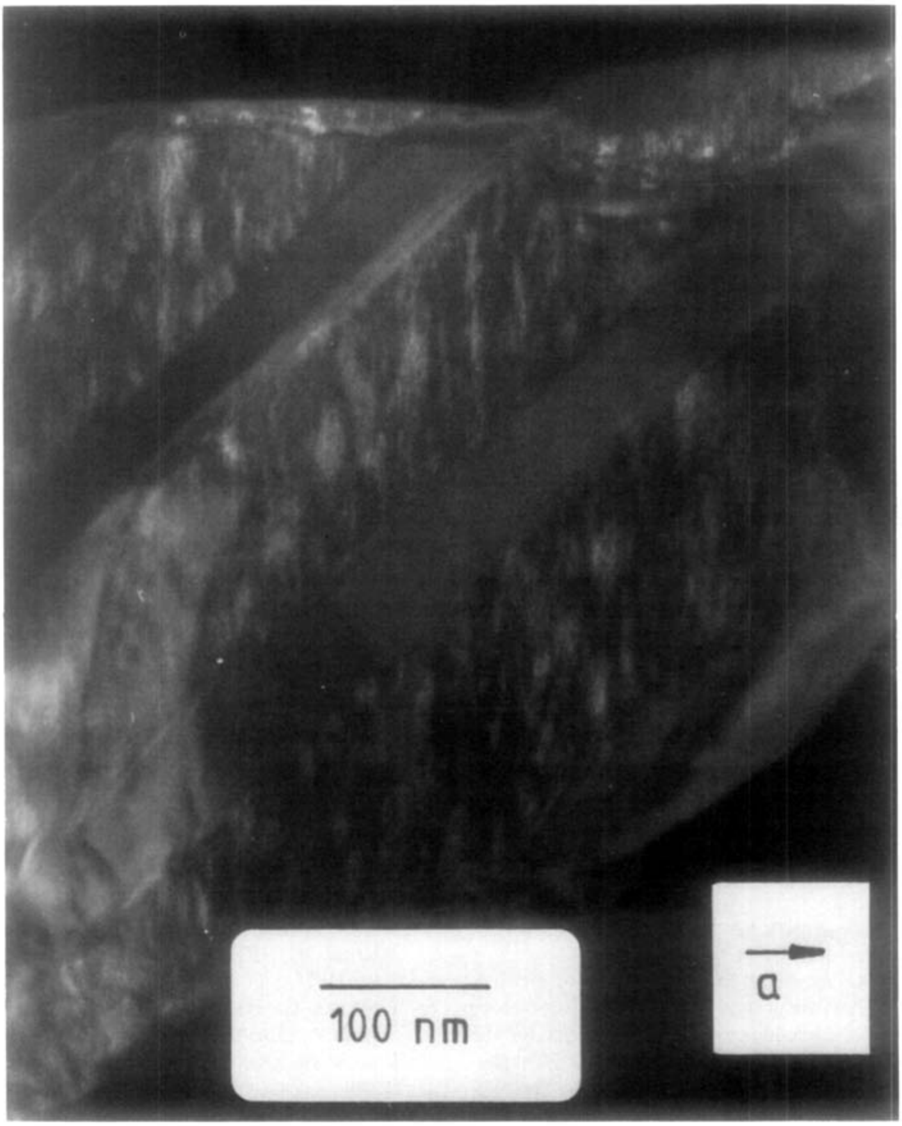

FIG. 7. Dark field image recorded using a ($\frac{1}{2}$ 0 0) reflection in $YBa_2Cu_3O_{6.6}$. The light areas inside one set of twins correspond to ordered regions.

Magnetic properties for both samples are shown in Fig. 8. Note that the transition is much sharper for the $x = 0.6$ than the $x = 0.5$ sample, and the Meissner fraction seems much larger. These results reflect the relative degree of superlattice ordering found in the two bulk samples by neutron diffraction and electron microscopy.

Conclusions

We have carried out neutron diffraction and electron microscopy examination of carefully prepared samples of $YBa_2Cu_3O_{6.5}$ and $YBa_2Cu_3O_{6.6}$. Both techniques show that the $a' = 2a$ supercell was less well developed in $YBa_2Cu_3O_{6.5}$. This variation in

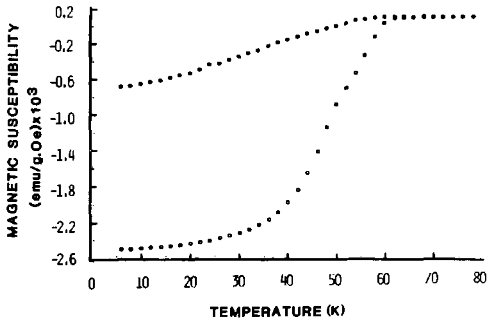

FIG. 8. Magnetic susceptibility curves for $YBa_2Cu_3O_{6.5}$ (solid circles) $YBa_2Cu_3O_{6.6}$ (open circles).

the degree of ordering is also reflected in the bulk Meissner effect measurements. For the bulk $YBa_2Cu_3O_{6.6}$ material, neutron diffraction shows a powder- and sample-average correlation distance of 26 Å in the a^* direction, while electron microscopy of selected crystals showed correlation lengths of ~100, ~200, and ~50 Å in the a^*, b^*, and c^* directions, respectively. Dark field imaging and neutron diffraction indicate a high volume fraction for the ordered domains of about 50%.

Acknowledgments

We thank G. Hewitson for the magnetic susceptibility data, M. Jewison of the David Dunlap Observatory for use of the microdensitometer, G. Pleizier for the preparation of $YBa_2Cu_3O_7$, and the Analytical Chemistry Section NRCC for trace element analysis. The Natural Science and Engineering Research Council of Canada and the Ontario Centre for Materials Research provided financial support.

References

1. R. J. Cava, B. Batlogg, C. H. Chen, E. A. Rietman, S. M. Zahurak, and D. Werder, *Nature (London)* **329,** 423 (1987).
2. R. Beyers, E. M. Engler, P. M. Grant, S. S. P. Parkin, G. Liu, M. L. Ramirez, K. P. Roche, J. E. Vazquez, V. Y. Lee, and R. D. Jocowitz, *Mater. Res. Soc. Symp. Proc.* **99,** 77 (1988).
3. D. J. Werder, C. H. Chen, R. J. Cava, and B. Batlogg, *Phys. Rev. B* **37,** 2317 (1988).
4. R. M. Fleming, L. F. Schneemeyer, P. K. Gallagher, B. Batlogg, L. W. Rupp, and J. V. Waszczak, *Phys. Rev. B* **37,** 7920 (1988).
5. C. H. Chen, D. J. Werder, L. F. Schneemeyer, P. K. Gallagher, and J. V. Waszczak, *Phys. Rev. B* **38,** 2888 (1988).
6. M. A. Alario-Franco, J. J. Capponi, C. Chaillout, J. Chenavas, and M. Marezio, *Mater. Res. Soc. Symp. Proc.* **99,** 41 (1988).
7. J. D. Jorgensen, H. Shaked, D. G. Hinks, B. Dabrowski, B. W. Veal, A. P. Paulikas, L. J. Nowicki, G. W. Crabtree, W. K. Kwok, and L. H. Nunez, *Physica C* **153–155,** 578 (1988).
8. A. Berera and D. de Fontaine, *Phys. Rev. B* **39,** 6727 (1989).
9. J. E. Greedan, A. O'Reilly, and C. V. Stager, *Phys. Rev. B* **35,** 8770 (1987).
10. P. B. Hirsch, A. Howie, R. B. Nicholson, D. W. Pashley, and M. J. Whelan, "Electron Microscopy of Thin Crystals," Krieger, New York (1977).
11. J. Reyes-Gasga, T. Krekels, G. Van Tendeloo, J. vanLanduyt, S. Amelincky, W. H. M. Bruggink, and H. Verweij, *Physica C* **159,** 831 (1989).